ACS APPLIED MATERIALS & INTERFACES

Research Article

www.acsami.org

Turn-on Fluorescent Sensing of Glutathione *S*-Transferase at near-Infrared Region Based on FRET between Gold Nanoclusters and Gold Nanorods

Long Qin,[†,‡] Xiwen He,[†,‡] Langxing Chen,*[,†,‡] and Yukui Zhang[†,‡,§]

[†]Research Center for Analytical Sciences, College of Chemistry, Tianjin Key Laboratory of Biosensing and Molecular Recognition, State Key Laboratory of Medicinal Chemical Biology, Nankai University, Tianjin 300071, China

[‡]Collaborative Innovation Center of Chemical Science and Engineering (Tianjin), Tianjin 300072, China

[§]Dalian Institute of Chemical Physics, Chinese Academy of Sciences, Dalian 116011, China

Supporting Information

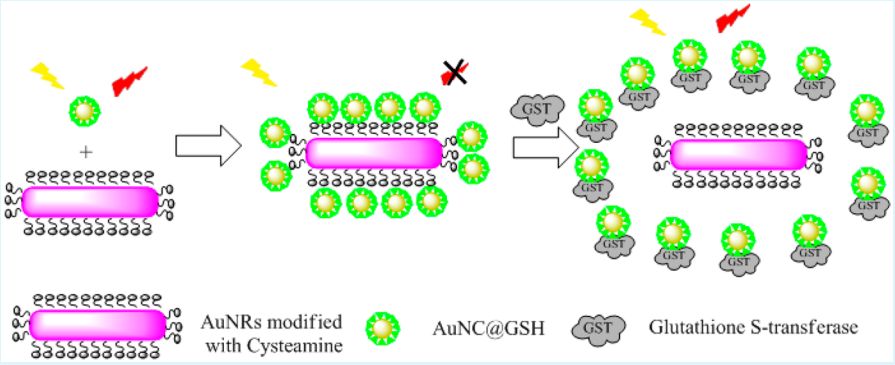

ABSTRACT: A fluorescence resonance energy transfer (FRET) method based on gold nanoclusters capped glutathione (AuNCs@GSH) and amine-terminated gold nanorods (AuNRs) is designed for turn-on and near-infrared region (NIR) sensing of glutathione *S*-transferase (GST). The absorption band of AuNRs is tuned carefully to maximize the spectra overlap and enhance the efficiency of FRET. The FRET from multiple AuNCs to single AuNR quenches about 70% fluorescence emission of AuNCs. After GST is added, the strong specific interaction of GSH−GST can replace the AuNCs@GSH from AuNRs, FRET based on electrostatic interaction between AuNCs@GSH and AuNRs is switched off. Thus, emission enhancement of AuNCs@GSH is observed. The fluorescent enhancement is linearly with the increasing GST concentration over the range of 2−100 nM GST and the limit of detection for GST is about 1.5 nM.

KEYWORDS: *fluorescence resonance energy transfer, gold nanoclusters, gold nanorods, glutathione S-transferase, near-infrared*

INTRODUCTION

Glutathione *S*-transferase (GST) is a family of cytosolic or membrane-bound multifunctional enzymes present in all organisms. GST protects cells against toxic chemicals in the human body such as endogenous superoxide radicals and toxic metabolites. GST is widely distributed in all organs of human beings,[1,2] but the concentration of GST in urine is extremely low. Appearance of enzyme proteins in urine represents renal disease or damage.[3] A previous report has shown that the concentration of GST in the urine of renal infraction patients could reach about 800 ng mL^{-1} for α-GST and 300 ng mL^{-1} for π-GST.[4] Therefore, GST is a suitable indicator for processes damaging the tubular epithelium of the kidney.[4,5] GST is also employed to tag recombinant proteins, which can be further purified by glutathione (GSH)-bound affinity chromatography making use of GSH−GST specific interaction.[6−8] A sandwich enzyme-linked immunosorbend assay (ELISA) method was presented for quantitative monitoring of recombinant fusion proteins containing GST.[9−11] Therefore, techniques to improve analytical methods including sensors based on nanomaterials to analyze GST or GST tagged protein quantitatively in complex samples have attracted considerable research efforts in recent years.[12−15]

Fluorescence resonance energy transfer (FRET), which occurs between two proximity molecules (donor and acceptor), is a potential alternative technology to investigate short distance-dependent interactions between the donor and acceptor.[16] In the past several years, there has been significant interest in the study of FRET between emerging nanomaterials and biomolecular recognition units, which has been proved to be an important strategy for applications in clinical diagnostics and biological assay.[17] Nanocrystal quantum dots (QDs) are

Received: January 10, 2015
Accepted: March 2, 2015
Published: March 2, 2015

DOI: 10.1021/acsami.5b00269
ACS Appl. Mater. Interfaces 2015, 7, 5965−5971

Scheme 1. Schematic Illustration of a Novel Turn-on Fluorescence Sensing System for the Detection of GST Based on the FRET between AuNCs and AuNRs in the NIR Region

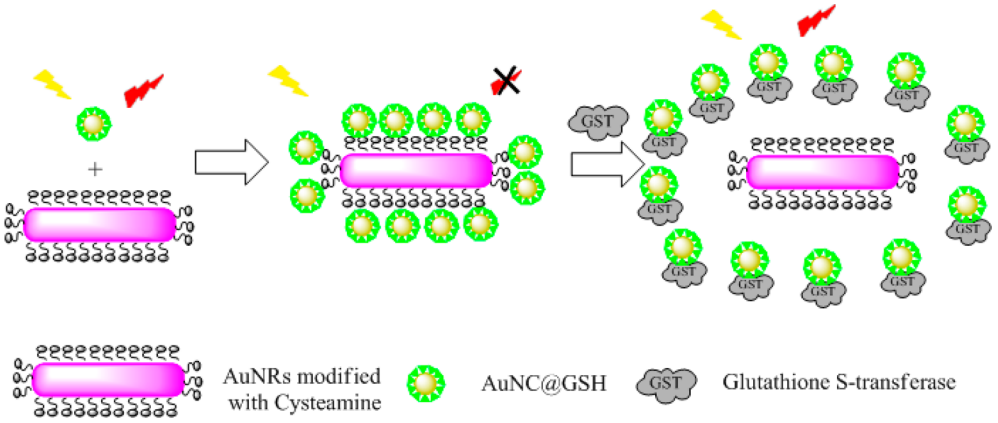

frequently used as fluorophores and have been proven to be effective FRET donors due to their broad absorption and narrow, symmetric emission. QDs-FRET based sensors have shown great promise in biological and environmental sensing.[18] In the design of QDs-FRET approaches, first, organic dyes[19−23] and Au nanoparticles (NPs)[24−30] are used as the acceptors. However, the organic dyes commonly suffer low photostability and the adsorption spectra of Au NPs with different sizes cannot be easily resolved, which results in the surface plasmon resonance peaks broaden with the increase of diameter at longer wavelength (above 650 nm). Compared with organic dyes or Au NPs, Au nanorods (AuNRs) have attracted much attention in biomedical applications such as biosensing, bioimaging, and photothermal therapy, due to their well-defined optical properties.[31] Due to their larger surface area, stronger optical absorption in the visible and near-infrared (NIR) region, AuNRs are suitable as a quenching acceptor for the FRET system, especially in the NIR region (650−1100 nm), which can increase the quenching sites and improve further the quenching efficiency. In recent years, much research has demonstrated that the near-infrared (NIR, 650−1100 nm) FRET system based on QDs and Au nanorods (AuNRs) is a potential alternative,[32−36] which can provide the possibility of high-efficiency energy transfer due to their high spectral overlap,[37−39] and the unique energy transfer mode of multiple donors and a single acceptor.[40,41] Unfortunately, applications of the QDs in biological, particularly for live cell imaging, are limited due to their high toxicity, large particle size upon functionalization, and tendency to aggregate.[42,43]

Recently, fluorescent metal nanoclusters (NCs), as a novel class of fluorophores, have received much attention.[44−48] Metal NCs are composed of a few to a hundred atoms, with sizes approaching to the Fermi wavelength of electrons, and exhibit discrete and size-tunable electronic transitions, thus leading to molecule-like properties such as strong fluorescence. Compared to QDs, Au NCs have fewer toxicity concerns. Au NCs have proved to be ideal fluorescence labels for biological applications and environmental monitoring and surveillance due to their attractive features including ultrasmall size (<2 nm), good biocompatibility, low-toxicity, and excellent photostability. Most fluorescence AuNCs sensors with the surface modification of receptors are single signal output, which is usually made on the basis of fluorescence quenching or recovery.[49] However, to the best of our knowledge, there is no report on FRET sensing with AuNCs−AuNRs bioconjugates in the NIR region.

In this work, we have developed a novel turn-on fluorescence sensing system for the detection of GST based on the FRET between AuNCs and AuNRs in the NIR region (Scheme 1). The FRET efficiency is related to the spectral overlap of the acceptor's absorption with the donor's emission, and inversely proportional to the sixth power of the distance between donor and acceptor.[40] Therefore, we choose AuNCs protected by GSH (AuNCs@GSH) as fluorescence donors and amine-terminated AuNRs as acceptors to form the FRET system. AuNCs@GSH can combine with positively charged AuNRs via electrostatic interaction and be further replaced by GST based on the specific interaction between GSH and GST. The absorption peak of AuNRs is tuned to the NIR range to maximize the overlap of the fluorescence emission of AuNCs. To improve the effect on the energy transfer, short-chain cysteamine is further modified on the surface of AuNRs. The AuNRs and AuNCs@GSH interact with each other via electrostatic attractive. FRET assembly is formed from AuNCs to AuNRs, leading to a 70% fluorescence quenching. Because the specific combination of GSH−GST is much stronger than the amine-carboxyl electrostatic interaction, the added GST can replace the AuNCs from AuNRs and switch off the FRET. The gradual emission enhancement of AuNCs is observed with increasing amount of GST. The detection limit of this approach for GST sensing is 1.5 nM. To the best of our knowledge, NIR and turn-on sensing of GST using AuNCs and AuNRs FRET probes has not been reported.

EXPERIMENTAL SECTION

Materials. $HAuCl_4 \cdot 3H_2O$ and hexadecyltrimethylammonium bromide (CTAB) were purchased from J&K Chemical; GSH and GST were purchased from Sigma-Aldrich. L-Ascorbic acid sodium salt was acquired from Alfa Aesar. Bovine serum albumin (BSA), bovine hemoglobin (BHb), ovalbumin egg (OVA), cytochrome C (Cyt C), and lysozyme (Lyz) were purchased from Solarbio. $NaBH_4$, $AgNO_3$, and other metal salts were obtained from Shanghai ShenXiang Chemical Reagent Co., Ltd.

Instrumentation. Fluorescence spectra were obtained from a Hitachi F-4500 fluorescence spectrofluorometer. The UV−visible spectra were recorded by a SHIMADZU UV-2450 UV−visible spectrophotometer. Transmission electron microscopy (TEM) images were obtained from a Tecnai G2 F20 transmission electron microscope. Determination of the ζ-potential of AuNRs and AuNCs in PB buffer (10 mM, pH 7.4) was performed on a Malvern Zetasizer 3000HSa (He−Ne laser, λ = 632.8 nm).

Synthesis of AuNCs@GSH. AuNCs@GSH was synthesized in one step based on a protocol described previously with slight

DOI: 10.1021/acsami.5b00269
ACS Appl. Mater. Interfaces 2015, 7, 5965−5971

modification.[50] Briefly, 3.0 mL of 10.0 mM $HAuCl_4$ was diluted with 4.15 mL of water. Then, 2.85 mL of 10.0 mM GSH was injected into the $HAuCl_4$ solution at 90 °C under vigorous stirring for 50 min. The resulting solution was centrifuged at 12 000 rpm for 30 min to remove large particles. The supernatant was then dialyzed for 2 days to remove the nonreactive species. The resultant solution was dried under vacuum and then redispersed in 10.0 mL of 10.0 mM pH 7.4 PB buffer.

Synthesis and Modification of AuNRs. AuNRs were prepared by a seed-mediated, Ag(I)-assisted growth method with slight modifications.[51] Briefly, the colloidal gold seed solution was prepared by mixing 0.25 mL of 10.0 mM $HAuCl_4$ solution with 9.75 mL of 0.1 M CTAB. Then, 0.6 mL of a freshly prepared ice-cold aqueous solution of 0.01 M $NaBH_4$ was added. The resultant solution was rapidly stirred for 2 min, and then kept for at 30 °C before use. After 2 h, 12.0 μL of the prepared gold seed solution was injected into a growth solution of 9.5 mL of 0.1 M CTAB, 0.5 mL of 0.01 M $HAuCl_4$, different volumes (35/70/105/140/175/210 μL) of 10.0 mM $AgNO_3$, and 55.0 μL of 0.1 M L-ascorbic acid. After seed addition, the growth solution was kept at 30 °C for 24 h. The AuNRs were purified by several cycles of centrifugation to remove excess CTAB. The precipitate was redispersed in 10.0 mL of 10.0 mM pH7.4 PB solution. The concentration of AuNRs is calculated as 2.5×10^{-10} M based on a previous report.[52]

The prepared AuNRs were modified with cysteamine based on the literature.[53] Specifically, 10.0 mL of AuNRs solution was mixed with 0.2 mL of 20.0 mM cysteamine under vigorous stirring. The mixture solution was sonicated for 30 min and then rapidly stirred for another 3 h at 50 °C. The resultant amine-terminated AuNRs were purified by several cycles of centrifugation, and the precipitate was then redispersed carefully with 10.0 mL of 10.0 mM pH 7.4 PB solution.

Fluoescence Quenching of AuNCs@GSH with Increasing AuNRs. 100.0 μL of the purified AuNCs and series amounts of amine-terminated AuNRs were mixed in a 2 mL centrifugal tube. The mixture was diluted to 400.0 μL with 10.0 mM pH 7.4 PB solution. 10 min later, the fluorescence spectra of these mixture solutions were recorded at an excitation wavelength of 590 nm

Sensing of GST based on AuNCs@GSH−AuNRs Assembly. 100.0 μL of AuNCs@GSH and 60.0 μL of prepared amine-terminated AuNRs were mixed in a 2 mL centrifugal tube. Various amounts of GST were then injected into the mixture solution separately after 10 min. The resultant solution was diluted to 400.0 μL with 10.0 mM pH 7.4 PB solution. The fluorescence spectra of these mixture solutions were recorded at an excitation wavelength of 590 nm after 15 min.

Procedures for monitoring GST in real samples. 100.0 μL of AuNCs and 60.0 μL of amine-terminated AuNRs were mixed in a 2 mL centrifugal tube. Different amounts of GST were first mixed with urine sample (40.0 μL). Then the urine sample was added to the AuNCs−AuNRs assembly solution. The resultant solution was diluted to 400.0 μL with 10.0 mM pH 7.4 PB solution. 15 min later, the fluorescence spectra of these mixture solutions were recorded at an excitation wavelength of 590 nm.

RESULTS AND DISCUSSION

Water-soluble luminescent of fluorescent AuNCs of high quality and uniformity have been synthesized by various methods.[44,47] In this work, GSH-protected AuNCs were prepared based on a previously proposed method.[50] The mean diameter of water-soluble GSH-protected AuNCs is ca. 2.4 ± 0.3 nm (Figure S1, Supporting Information). Although it is difficult to measure the surface density of GSH in AuNCs@GSH and cystamine in Au NRs in the AuNCs−AuNRs assembly, the influence of the molar ratio of GSH to $HAuCl_4$ on the fluorescence emission of AuNCs@GSH was investigated. If the molar ratio of GSH to $HAuCl_4$ was low, the synthesized AuNCs had poor stability. As can be seen from Figure 1, the intensity of fluorescence emission of AuNCs@GSH increased along with the increase of molar ratio of GSH

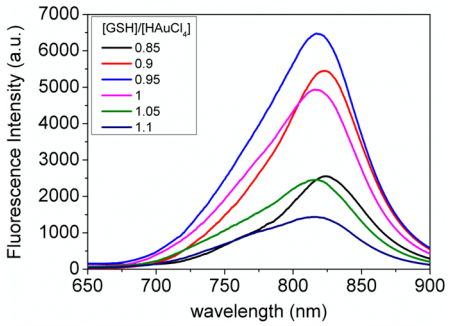

Figure 1. Emission spectra of AuNCs@GSH in the molar ratios of [GSH]/[$HAuCl_4$] from 0.85:1 to 1.1:1.

to $HAuCl_4$ from 0.85:1 to 0.95:1 and AuNCs@GSH has the maximum emission in the presence of a molar ratio of GSH to $HAuCl_4$ of 0.95:1. When the molar ratio of GSH to $HAuCl_4$ is further increased to 1.1:1, the intensity of fluorescence emission of AuNCs@GSH diminishes on the contrary and the blue shift of fluorescence emission peak was observed. The product of AuNCs@GSH in the molar ratio of GSH to $HAuCl_4$ of 0.95:1 has fluorescence emission bands centered at 824 nm, with an excitation wavelength at 590 nm (Figure 1). The quantum yield (QY) of AuNCs is about 1.0% in 10.0 mM pH 7.4 PB solution, which is similar to that of a previous report.[50]

AuNRs have two localized surface plasma resonance (LSPR) modes, one is the longitudinal LSPR mode associated with the electron oscillations along the length axis, the other is the transverse LSPR mode excited by light polarized along the transverse direction of the nanorod. The plasmon wavelength of the longitudinal mode can be synthetically turned across a broad spectral range, covering the visible and near-infrared (NIR) regions by tailoring their aspect ratio (length to diameter) to accommodate different applications.[39,54−57] Due to the high extinction coefficient and tunable strong longitudinal absorption peak, AuNRs are chosen to be the quencher of the AuNCs−AuNRs FRET system. To increase the efficiency of the FRET process, the distance between donor and acceptor must be decreased, so AuNRs were modified with thiol-molecular cysteamine because of its positive charge and short length. To control the aspect ratio and longitudinal absorption peak of AuNRs, the effect of $AgNO_3$ content was investigated. As shown in Figure S2 (Supporting Information), the longitudinal absorption peak shows great red shift with the increase of $AgNO_3$ concentration, which confirms the result of a previous report.[54] When the 140.0 μM $AgNO_3$ was added into the reaction mixture, the maximal wavelength of the longitudinal absorption was displayed at 875 nm. After the modification of cysteamine, a large blue shift of about 50 nm of the absorption peak is observed. The maximal wavelength of the longitudinal absorption of AuNRs was shifted from 875 to 822 nm. A more severe degree of blue shift was observed for further increasing the concentration of cysteamine. The amount of cysteamine was the optimal concentration to maximize the spectra overlap and enhance the quenching efficiency. To improve the efficiency of our FRET system, 140.0 μM $AgNO_3$ is selected to maximize the spectra overlap between quenchers (822 nm for AuNRs) and donors (824 nm for AuNCs) (Figure 2). The longitudinal absorption peak is very sensitive to the morphology of AuNRs and can be tuned from 600 to 1300 nm by their aspect ratio. In this work, TEM image of the amine-terminated AuNRs in FRET system is shown in Figure S3

DOI: 10.1021/acsami.5b00269
ACS Appl. Mater. Interfaces 2015, 7, 5965−5971

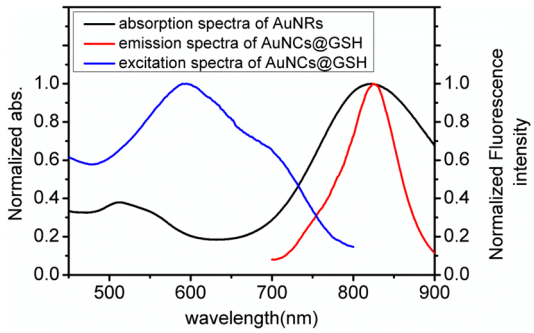

Figure 2. Normalized SPR absorption spectra of amine-terminated AuNRs and excitation/emission spectra of AuNCs@GSH. The emission spectrum was measured at λ_{ex} = 590 nm, and the excitation spectrum was measured at λ_{em} = 824 nm.

(Supporting Information). The size of AuNRs is 15 ± 1 nm as diameter and 56 ± 9 nm as length, with aspect ratio of 3.7. The synthesized AuNRs are well dispersed in PB buffer (pH 7.4), and the color of the AuNRs solution displays pink. The concentration of AuNRs is calculated as 2.5×10^{-10} M based on a previous report.[52]

The ζ-potential of amine-terminated AuNRs and AuNCs@GSH has been measured. The value of AuNRs was +42.2 mV, which is similar to that of a previous report.[32] The ζ-potential of AuNCs@GSH was measured as −18.6 mV. As the positively charged AuNRs was introduced to the negatively charged AuNCs@GSH solution, AuNCs were attracted on the surface of AuNRs and a hybrid system was formed based on the electrostatic interaction. As can be seen from the TEM image in Figure 3a, there are more than 20 AuNCs attracted at the sides of single AuNR. So, it is reasonable to estimate that single AuNR is surrounded by more than 40 AuNCs, which is consistent with the AuNR−QDs assembly (each AuNR surrounded by more than 40 QDs).[32] The distance between the surface of the AuNRs and the inner layer of the AuNCs was about 1.7 nm, so the high efficiency of the FRET could be established at this short distance. Multiple AuNCs are attracted to the AuNCs−AuNRs assembly, which could enhance the FRET efficiency. As expected, the emission of AuNCs@GSH is quenched with increasing concentration of AuNRs. The fluorescent quenching of AuNCs@GSH is ascribed to the energy transfer from AuNCs to AuNRs. The required time of the quenching process was also investigated. From Figure S4 of the Supporting Information, a steady state of fluorescence emission can be observed within 10 min. The estimated FRET efficiency is defined as $E = 1 - F_{DA}/F_D$, where F_{DA} and F_D are the fluorescence intensities of the donor in the presence and absence of acceptor. As shown in Figure 3b, the FRET efficiency could reach about 70% after 60.0 μL of AuNRs was injected into 100.0 μL of AuNCs solution. The high energy transfer efficiency is attributed to the following reasons. First, the most important reason is the close proximity of AuNRs to AuNCs,[32] because FRET efficiency is inversely proportional to the sixth-power of the distance between donor and acceptor. Second, AuNRs have the stronger optical absorption, and the extinction coefficient of AuNRs is more than 10^9 M^{-1} cm^{-1},[38,52] which can enhance the quenching effect. Finally, AuNRs have a larger surface area and higher surface energy, which can increase the quenching sites and improve further the quenching efficiency.[33−35,38]

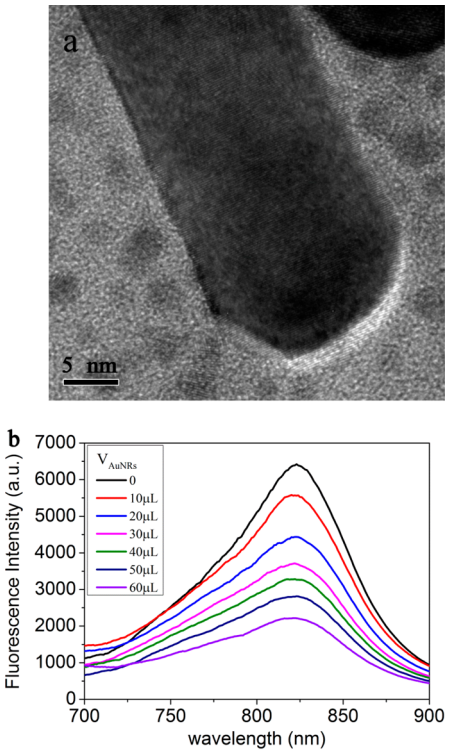

Figure 3. (a) TEM image of AuNCs−AuNRs assembly with mixture solution containing 100.0 μL of AuNCs and 60.0 μL of amine-terminated AuNRs. (b) Fluorescence spectra of AuNCs@GSH after addition of various amounts of AuNRs. The volumes of AuNRs from top to bottom are 0, 10, 20, 30, 40, 50, and 60 μL.

The effect of pH on the AuNCs−AuNRs assembly in 10 mM PB buffer was investigated. As shown in Figure S5 of the Supporting Information, no obvious effect of pH value to the quenched emission of AuNCs−AuNRs assembly and the restored fluorescent of AuNCs is observed, indicating that the interaction of the amine and carboxyl groups is rather strong. The AuNCs−AuNRs assembly used in this system is stable in 10 mM PB buffer at pH 7.4.

After GST is introduced to the AuNCs@GSH−AuNRs mixture solution, as expected, a gradual recovery of the quenched emission is observed with increasing concentration of GST to about 100 nM. Previous work has reported that AuNCs and AuNPs protected by GSH can bind with GST via GSH−GST specific interaction.[13,14] Because the GSH−GST specific interaction is stronger than the electrostatic interaction between AuNCs@GSH and AuNRs, the electrostatic interaction is broken after the AuNCs@GSH bind specifically with GST. Therefore, FRET process from AuNCs@GSH to AuNRs is switched off due to the increased distance between donor and acceptor.

The interaction of AuNCs@GSH with different concentrations of GST is also investigated. The effect of GST on the emission of AuNCs@GSH is shown in Figure 4. We did not observe a change of the emission intensity of AuNCs when the concentration of GST in the mixture was lower than 1 μM. As shown in the TEM image of Figure S6 (Supporting Information), AuNCs could be still well dispersed in the presence of 1 μM GST. However, a huge decrease on the emission of AuNCs was found with 10 μM GST. Therefore, the concentration of GST in this sensing strategy can be detected less than 1 μM.

DOI: 10.1021/acsami.5b00269
ACS Appl. Mater. Interfaces 2015, 7, 5965−5971

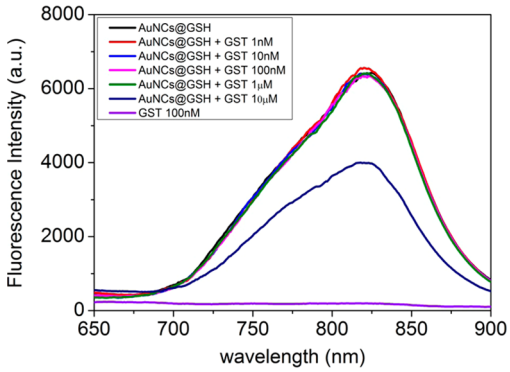

Figure 4. Fluorescence emissions of AuNCs after addition of different concentrations of GST from 1 nM to 10 μM.

To explore the feasibility of this approach for quantitative analysis of GST, we investigate the response of AuNCs−AuNRs assemblies toward the concentration of GST. As shown in Figure 5, the concentration curve is linear from 2 to 100 nM

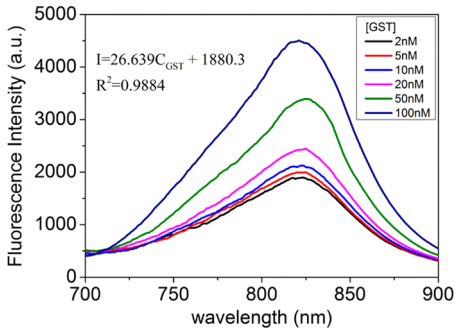

Figure 5. Fluorescence spectra of AuNCs−AuNRs assembly with addition of GST. The concentrations of GST from bottom to top are 2, 5, 10, 20, 50, and 100 nM.

for GST (I = 26.639C_{GST} + 1880.3, R^2 = 0.9884). The detection limit (LOD) for GST at a signal-to-noise ratio of 3 is estimated to be 1.5 nM. As the concentration of GST is higher than 100 nM, little fluorescence recovery of the AuNCs−AuNRs system can be observed. At a higher concentration range, the quenching effect of GST to the emission of AuNCs cannot be negligent. Although the fluorescence intensity of AuNCs is still improved by the broken FRET process, the emission signal is quenched by the high concentration of GST at the same time.

To investigate the selectivity of the FRET approach, five standard proteins, BSA, BHb, OVA, Cyt C, and Lyz, are used as interfering proteins to test the fluorescence response of the AuNCs−AuNRs system. As shown in Figure 6a, no recovery responses are observed as the concentration of each interfering protein is 1 μM. Enhancement of fluorescence signal is found only when GST (100 nM) is introduced. We then assess the influence of metal ions (Na^+, K^+, Ag^+,Ca^{2+},Mg^{2+}, Zn^{2+}, Co^{2+},Cu^{2+}, Fe^{3+}, Ba^{2+}, Cd^{2+}, Mn^{2+}, Ni^{2+}, and Pb^{2+}) on our present method. As shown in Figure 6b, 1 μM metal ions have no obvious influence on this approach for GST sensing. The complex of two GSH with single Cu^{2+} could induce aggregation and fluorescence quenching of AuNCs@GSH.[50,58] A similar phenomenon of fluorescence quenching was observed when Cu^{2+} was introduced to an individual AuNCs@GSH solution in our experiment. However, as the AuNCs−AuNRs assembly was

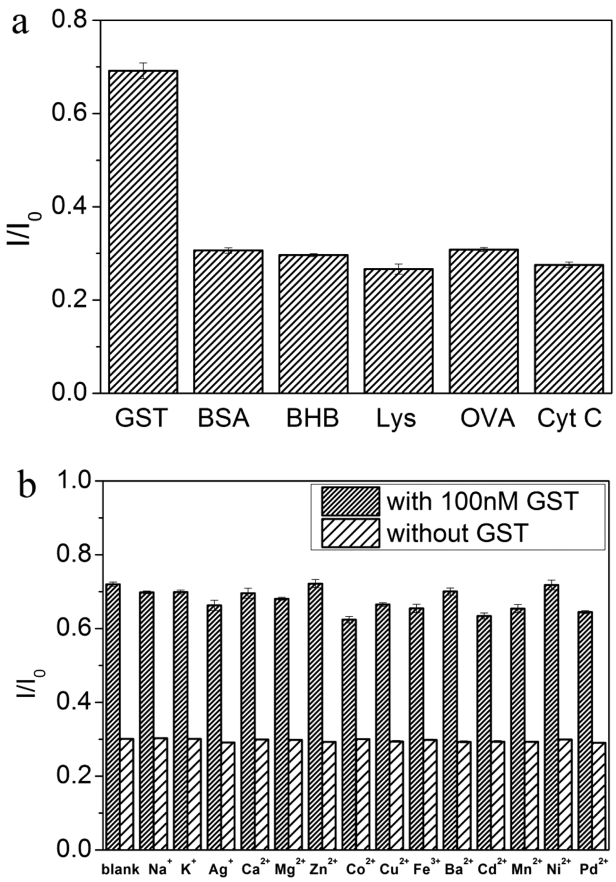

Figure 6. (a) Fluorescence intensity of AuNCs−AuNRs assembly with introduction of different proteins. The concentration of GST is 100 nM, whereas those of other proteins are 1 μM. I_0 is the fluorescence intensity of individual AuNCs@GSH. (b) Fluorescence intensity of AuNCs−AuNRs probe with introduction of various metal ions (Na^+, K^+, Ag^+, Ca^{2+},Mg^{2+}, Zn^{2+}, Co^{2+}, Cu^{2+}, Fe^{3+}, Ba^{2+}, Cd^{2+}, Mn^{2+}, Ni^{2+}, and Pb^{2+}). The concentrations of these metal ions are 1 μM. I_0 is the fluorescence intensity of individual AuNCs@GSH.

formed, multiple AuNCs@GSH were attracted on the surface of AuNRs, and FRET from AuNCs to AuNRs quenched approximately 70% fluorescence emission of AuNCs. Therefore, no fluorescence quenching of AuNCs−AuNRs assembly was observed by the addition of Cu^{2+}. When the AuNCs−AuNRs FRET assembly was switched off by GST, multiple GST could connect to the surface of AuNCs@GSH. The strong interaction of GSH−GST and steric hindrance of GST at the surface of AuNCs@GSH could protect AuNCs@GSH from aggregation. Due to the GSH−GST specific interaction, our FRET approach shows good selectivity.

Additionally, the potential application of the AuNCs−AuNRs assembly is investigated. The sensing of urine GST is detected. Urine samples of healthy volunteers with addition of GST are used to simulate urine of renal damage patients. As shown in Figure S7 of the Supporting Information, recovery of fluorescence emission is only found when GST is introduced. No response of the emission signal is observed in diluted urine without GST. These results demonstrate that our approach has sensing potential for GST in urine samples.

CONCLUSIONS

In conclusion, we have demonstrated that the AuNCs−AuNRs hybrid probe can be used for turn-on sensing of GST in the

DOI: 10.1021/acsami.5b00269
ACS Appl. Mater. Interfaces 2015, 7, 5965−5971

NIR region. The FRET from AuNCs@GSH to amine-terminated AuNRs can be switched off by the specific interaction of GSH−GST, with a detection limit of 1.5 nM for GST. High selectivity is also guaranteed by this specific interaction. To the best of our knowledge, this is the first report on using a AuNCs−AuNRs probe for turn-on and NIR sensing to detect GST. The strategy of this work is promising to develop a general sensing method making use of the stronger specific interaction of affinity ligands for more analytes

■ ASSOCIATED CONTENT

Supporting Information

TEM images of the AuNCs@GSH, TEM image of amine-terminated AuNRs, SPR absorption spectra of AuNRs, fluorescence spectra of AuNCs−AuNRs assembly, and the effect of pH on the fluorescence of AuNCs−AuNRs assembly. This material is available free of charge via the Internet at http://pubs.acs.org/.

■ AUTHOR INFORMATION

Corresponding Author

*L. Chen. Fax: (+86) 22-2350-2458. E-mail: lxchen@nankai.edu.cn.

Notes

The authors declare no competing financial interest.

■ ACKNOWLEDGMENTS

The authors are grateful to the National Basic Research Program of China (No. 2012CB910601), the National Natural Science Foundation of China (Nos. 21275080, 21475067), and the Research Fund for the Doctoral Program of Higher Education of China (No. 20120031110007).

■ REFERENCES

(1) Faulder, C. G.; Hirrell, P. A.; Hume, R.; Strange, R. C. Studies of the Development of Basic, Neutral and Acidic Isoenzymes of Glutathione S-Transferase in Human Liver, Adrenal, Didney and Spleen. *Biochem. J.* **1987**, *241*, 221−228.

(2) Corrigall, A. V.; Kirsch, R. E. Glutathione S-TransferaseDistribution and Concentration in Human Organs. *Biochem. Int.* **1988**, *16*, 443−448.

(3) Feinfeld, D. A.; Sherman, R. A.; Safirstein, R.; Ohmi, N.; Fuh, V. L.; Arias, I. M.; Levine, S. D. Urinary Ligandin in Renal Tubular Cell Injury. *Contrib. Nephrol.* **1984**, *42*, 111−117.

(4) Sundberg, A. G. M.; Nilsson, R.; Appelkvist, E. L.; Dallner, G. ELISA Procedures for the Quantitation of Glutathione Transferases in the Urine. *Kidney Int.* **1995**, *48*, 570−575.

(5) Holmquist, P.; Liuba, P. Urine α-Glutathione S-Transferase, Systemic Inflammation and Arterial Function in Juvenile Type 1 Diabetes. *J. Diabetes Complications* **2012**, *26*, 199−204.

(6) Di Ilio, C.; Aceto, A.; Piccolomini, R.; Allocati, N.; Faraone, A.; Bucciarelli, T.; Barra, D.; Federici, G. Purification and Characterization of a Novel Glutathione Transferase from *Serratia marcescens*. *Biochim. Biophys. Acta* **1991**, *1077*, 141−146.

(7) Hsieh, C. H.; Liu, L. F.; Tsai, S. P.; Tam, M. F. Characterization and Cloning of Avian-Hepatic Glutathione S-Transferases. *Biochem. J.* **1999**, *343*, 87−93.

(8) Harris, J. M.; Meyer, D. J.; Coles, B.; Ketterer, B. A Novel Glutathione Transferase (13-13) Isolated from the Matrix of Rat Liver Mitochondria Having Structural Similarity to Class Theta Enzymes. *Biochem. J.* **1991**, *278*, 137−141.

(9) Rabin, D. U.; Palmer-Crocker, R.; Mierz, D. V.; Yeung, K. K. An ELISA Sandwich Capture Assay for Recombinant Fusion Proteins Containing Glutathione-S-Transferase. *J. Immunol. Methods* **1992**, *156*, 101−105.

(10) Mulder, T. P. J.; Peters, W. H. M.; Court, D. A.; Jansen, J. B. M. J. Sandwich ELISA for Glutathione S-Transferase Alpha 1-1: Plasma Concentrations in Controls and in Patients with Gastrointestinal Disorders. *Clin. Chem.* **1996**, *42*, 416−419.

(11) Ha, T. H.; Jung, S. O.; Lee, J. M.; Lee, K. Y.; Lee, Y.; Park, J. S.; Chung, B. H. Oriented Immobilization of Antibodies with GST-Fused Multiple Fc-Specific B-Domains on a Gold Surface. *Anal. Chem.* **2007**, *79*, 546−556.

(12) Espinoza, H. M.; Shireman, L. M.; McClain, V.; Atkins, W.; Gallagher, E. P. Cloning, Expression and Analysis of the Olfactory Glutathione S-Transferases in Coho Salmon. *Biochem. Pharmacol.* **2013**, *85*, 839−848.

(13) Zheng, M.; Huang, X. Y. Nanoparticles Comprising a Mixed Monolayer for Specific Bindings with Biomolecules. *J. Am. Chem. Soc.* **2004**, *126*, 12047−12054.

(14) Chen, C. T.; Chen, W. J.; Liu, C. Z.; Chang, L. Y.; Chen, Y. C. Glutathione-Bound Gold Nanoclusters for Selective-Binding and Detection of Glutathione S-Transferase-Fusion Proteins from Cell Lysates. *Chem. Commun.* **2009**, 7515−7517.

(15) Shin, Y. B.; Lee, J. M.; Park, M. R.; Kim, M. G.; Chung, B. H.; Pyo, H. B.; Maeng, S. Analysis of Recombinant Protein Expression Using Localized Surface Plasmon Resonance (LSPR). *Biosens. Bioelectron.* **2007**, *22*, 2301−2307.

(16) Sapsford, K. E.; Berti, L.; Medintz, I. L. Materials for Fluorescence Resonance Energy Transfer Analysis: Beyond Traditional Donor-Acceptor Combinations. *Angew. Chem., Int. Ed.* **2006**, *45*, 4562−4568.

(17) Wu, B. Y.; Wang, H. F.; Chen, J. T.; Yang, X. P. Fluorescence Resonance Energy Transfer Inhibition Assay for α-Fetoprotein Excreted during Cancer Cell Growth Using Functionalized Persistent Luminescence Nanoparticles. *J. Am. Chem. Soc.* **2011**, *133*, 686−688.

(18) Gill, R.; Zayats, M.; Willner, I. Semiconductor Quantum Dots for Bioanalysis. *Angew. Chem., Int. Ed.* **2008**, *47*, 7602−7625.

(19) Shi, L. F.; Paoli, V. D.; Rosenzweig, N.; Rosenzweig, Z. Synthesis and Application of Quantum Dots FRET-based Protease Sensors. *J. Am. Chem. Soc.* **2006**, *128*, 10378−10379.

(20) Shi, L. F.; Rosenzweig, N.; Rosenzweig, Z. Luminescent Quantum Dots Fluorescence Resonance Energy Transfer-based Probes for Enzymatic Activity and Enzyme Inhibitors. *Anal. Chem.* **2007**, *79*, 208−214.

(21) Crivat, G.; Da Silva, S. M.; Reyes, D. R.; Locascio, L. E.; Gaitan, M.; Rosenzweig, N.; Rosenzweig, Z. Quantum Dot FRET-based Probes in Thin Films Grown in Microfluidic Channels. *J. Am. Chem. Soc.* **2010**, *132*, 1460−1461.

(22) Medintz, I. L.; Pons, T.; Sasumu, K.; Boeneman, K.; Dennis, A. M.; Farrell, D.; Deschamps, J. R.; Melinger, J. S.; Bao, G.; Mattoussi, H. Resonance Energy Transfer between Luminescent Quantum Dots and Diverse Fluorescent Protein Acceptors. *J. Phys. Chem. C* **2009**, *113*, 18552−18561.

(23) Boeneman, K.; Delehanty, J. B.; Sasumu, K.; Stewart, M. H.; Medintz, I. L. Intracellular Bioconjugation of Targeted Proteins with Semiconductor Quantum Dots. *J. Am. Chem. Soc.* **2010**, *132*, 5975−5977.

(24) Wang, D. Y.; Rogach, A. L.; Caruso, F. Semiconductor Quantum Dot-Labeled Microsphere Bioconjugates Prepared by Stepwise Self-Assembly. *Nano Lett.* **2002**, *2*, 857−861.

(25) Chang, E.; Miller, J. S.; Sun, J. T.; Yu, W. W.; Colvin, V. L.; Drezek, R.; West, J. L. Protease-Activated Quantum Dot Probes. *Biochem. Biophys. Res. Commun.* **2005**, *334*, 1317−1321.

(26) Oh, E.; Hong, M. Y.; Lee, D.; Nam, S. H.; Yoon, H. C.; Kim, H. S. Inhibition Assay of Biomolecules Based on Fluorescence Resonance Energy Transfer (FRET) between Quantum Dots and Gold Nanoparticles. *J. Am. Chem. Soc.* **2005**, *127*, 3270−3271.

(27) Pons, T.; Medinz, I. L.; Sapsford, K. E.; Higashiya, S.; Grimes, A. F.; English, D. S.; Mattoussi, H. On the Quenching of Semiconductor Quantum Dot Photoluminescence by Proximal Gold Nanoparticles. *Nano Lett.* **2007**, *7*, 3157−3164.

(28) Shan, Y.; Xu, J. J.; Chen, H. Y. Distance-Dependent Quenching and Enhancing of Electrochemiluminescence from a CdS:Mn

DOI: 10.1021/acsami.5b00269
ACS Appl. Mater. Interfaces 2015, 7, 5965−5971

Nanocrystal Film by Au Nanoparticles for Highly Sensitive Detection of DNA. *Chem. Commun.* **2009**, 905−907.
(29) Quach, A. D.; Crivat, G.; Tarr, M. A.; Rosenzweig, Z. Gold Nanoparticle-Quantum Dot-Polystyrene Microspheres as Fluorescence Resonance Energy Transfer Probes for Bioassays. *J. Am. Chem. Soc.* **2011**, *133*, 2028−2030.
(30) Wargnier, R.; Baranov, A. V.; Maslov, V. G.; Stsiapura, V.; Artemyev, M.; Pluot, M.; Sukhanova, A.; Nabiev, I. Energy Transfer in Aqueous Solutions of Oppositely Charged CdSe/ZnS Core/Shell Quantum Dots and in Quantum Dot-Nanogold Assemblies. *Nano Lett.* **2004**, *4*, 451−457.
(31) Chen, H. J.; Shao, L.; Li, Q.; Wang, J. F. Gold Nanorods and Their Plasmonic Properties. *Chem. Soc. Rev.* **2013**, *42*, 2679−2724.
(32) Xia, Y. S.; Song, L.; Zhu, C. Q. Turn-on and near-Infrared Fluorescent Sensing for 2,4,6-Trinitrotoluene Based on Hybrid (Gold Nanorod)-(Quantum Dots) Assembly. *Anal. Chem.* **2011**, *83*, 1401−1407.
(33) Li, X.; Qian, J.; Jiang, L.; He, S. L. Fluorescence Quenching of Quantum Dots by Gold Nanorods and its Application to DNA Detection. *Appl. Phys. Lett.* **2009**, *94*, 063111−063113.
(34) Liang, G. X.; Pan, H. C.; Li, Y.; Jiang, L. P.; Zhang, J. R.; Zhu, J. J. Near Infrared Sensing Based on Fluorescence Resonance Energy Transfer between Mn:CdTe Quantum Dots and Au Nanorods. *Biosens. Bioelectron.* **2009**, *24*, 3693−3697.
(35) Zeng, Q. H.; Zhang, Y. L.; Liu, X. M.; Tu, L. P.; Kong, X. G.; Zhang, H. Multiple Homogeneous Immunoassays Based on a Quantum Dots-Gold Nanorods FRET Nanoplatform. *Chem. Commun.* **2012**, 1781−1783.
(36) Agarwal, A.; Lilly, G. D.; Govorov, A. O.; Kotov, N. A. Optical Emission and Energy Transfer in Nanoparticle-Nanorod Assemblies: Potential Energy Pump System for Negative Refractive Index Materials. *J. Phys. Chem. C* **2008**, *112*, 18314−18320.
(37) Bruchez, M. J.; Moronne, M.; Gin, P.; Weiss, S.; Alivisatos, A. P. Semiconductor Nanocrystals as Fluorescent Biological Labels. *Science* **1998**, *281*, 2013−2016.
(38) Nikoobakht, B.; Wang, J. P.; El-Sayed, M. A. Surface-Enhanced Raman Scattering of Molecules Adsorbed on Gold Nanorods: Off-Surface Plasmon Resonance Condition. *Chem. Phys. Lett.* **2002**, *366*, 17−23.
(39) Murphy, C. J.; Thompson, L. B.; Alkilany, A. M.; Sisco, P. N.; Boulos, S. P.; Sivapalan, S. T.; Yang, J. A.; Chernak, D. J.; Huang, J. Y. The Many Faces of Gold Nanorods. *J. Phys. Chem. Lett.* **2010**, *1*, 2867−2875.
(40) Medintz, I. L.; Clapp, A. R.; Mattoussi, H.; Goldman, E. R.; Fisher, B.; Mauro, J. M. Self-Assembled Nanoscale Biosensors Based on Quantum Dot FRET Donors. *Nat. Mater.* **2003**, *2*, 630−638.
(41) Haldar, K. K.; Sen, T.; Patra, A. Metal Conjugated Semiconductor Hybrid Nanoparticle-based Fluorescence Resonance Energy Transfer. *J. Phys. Chem. C* **2010**, *114*, 4869−4874.
(42) Derfus, A. M.; Chan, W. C. W.; Bhatia, S. N. Probing the Cytotoxicity of Semiconductor Quantum Dots. *Nano Lett.* **2004**, *4*, 11−18.
(43) Liu, J. M.; Chen, J. T.; Yan, X. P. Near Infrared Fluorescent Trypsin Stabilized Gold Nanoclusters as Surface Plasmon Enhanced Energy Transfer Biosensor and in Vivo Cancer Imaging Bioprobe. *Anal. Chem.* **2013**, *85*, 3238−3245.
(44) Shang, L.; Dong, S. J.; Nienhaus, G. U. Ultra-Small Fluorescent Metal Nanoclusters: Synthesis and Biological Applications. *Nano Today* **2011**, *6*, 401−408.
(45) Díez, I.; Ras, R. H. A. Fluorescent Silver Nanoclusters. *Nanoscale* **2011**, *3*, 1963−1970.
(46) Yuan, X.; Luo, Z. T.; Zhang, Q. B.; Zhang, X. H.; Zheng, Y. G.; Lee, J. Y.; Xie, J. P. Synthesis of Highly Fluorescent Metal (Ag, Au, Pt, and Cu) Nanoclusters by Electrostatically Induced Reversible Phase Transfer. *ACS Nano* **2011**, *5*, 8800−8808.
(47) Cui, M. L.; Zhao, Y.; Song, Q. J. Synthesis, Optical Properties and Applications of Ultra-Small luminescent Gold Nanoclusters. *TrAC, Trends Anal. Chem.* **2014**, *57*, 73−82.
(48) Zheng, J.; Nicovich, P. R.; Dickson, R. M. Highly Fluorescent Noble-Metal Quantum Dots. *Annu. Rev. Phys. Chem.* **2007**, *58*, 409−431.
(49) Wang, M.; Mei, Q. S.; Zhang, K.; Zhang, Z. P. Protein-Gold Nanoclusters for Identification of Amino Acids by Metal Ions Modulated Ratiometric Fluorescence. *Analyst* **2012**, *137*, 1618−1623.
(50) Tu, X. J.; Chen, W. B.; Guo, X. Q. Facile One-Pot Synthesis of near-Infrared Luminescent Gold Nanoparticles for Sensing Copper-(II). *Nanotechnology* **2011**, *22*, 095701−095707.
(51) Sau, T. K.; Murphy, C. J. Seeded High Yield Synthesis of Short Au Nanorods in Aqueous Solution. *Langmuir* **2004**, *20*, 6414−6420.
(52) Orendorff, C. J.; Murphy, C. J. Quantitation of Metal Content in the Silver-Assisted Growth of Gold Nanorods. *J. Phys. Chem. B* **2006**, *110*, 3990−3994.
(53) Wang, C. G.; Irudayaraj, J. Multifunctional Magnetic-Optical Nanoparticle Probes for Simultaneous Detection, Separation, and Thermal Ablation of Multiple Pathogens. *Small* **2010**, *6* (2), 283−289.
(54) Nikoobakht, B.; El-Sayed, M. A. Preparation and Growth Mechanism of Gold Nanorods (NRs) Using Seed-Mediated Growth Method. *Chem. Mater.* **2003**, *15*, 1957−1962.
(55) Murphy, C. J.; Gole, A. M.; Hundyadi, S. E.; Stone, J. W.; Sisco, P. N.; Alkilany, A.; Kinard, B. E.; Hankins, P. Chemical Sensing and Imaging with Metallic Nanorods. *Chem. Commun.* **2008**, 544−557.
(56) Huang, X. H.; Neretina, S.; El-Sayed, M. A. Gold Nanorods: From Synthesis and Properties to Biological and Biomedical Applications. *Adv. Mater.* **2009**, *21*, 4880−4910.
(57) Sau, T. K.; Rogach, A. L.; Jäckel, F.; Klar, T. A.; Feldmann, J. Properties and Applications of Colloidal Nonspherical Noble Metal Nanoparticles. *Adv. Mater.* **2010**, *22*, 1805−1825.
(58) Fang, C.; Zhou, X. Y. Voltammetry and EQCM Investigation of Glutathione Monolayer and Its Complexation with Cu^{2+}. *Electroanalysis* **2003**, *15*, 1632−1638.

DOI: 10.1021/acsami.5b00269
ACS Appl. Mater. Interfaces 2015, 7, 5965−5971